Research Square

Preprints are preliminary reports that have not undergone peer review.
They should not be considered conclusive, used to inform clinical practice,
or referenced by the media as validated information.

Human Responses to Graded Light Exposure in the Temporal Visual Field during Central Visual Tasks

Yaodong He
Northeast Forestry University
Bo Li
libo@nefu.edu.cn
Northeast Forestry University
Yufei Du
Northeast Forestry University
Laicheng Yin
Northeast Forestry University

Article

Keywords: Indoor lighting, Light exposure, Visual field, Cognitive performance, Psychophysiological responses

Posted Date: August 28th, 2026

DOI: https://doi.org/10.21203/rs.3.rs-10692445/v1

License: This work is licensed under a Creative Commons Attribution 4.0 International License. Read Full License

Additional Declarations: No competing interests reported.

Abstract

Indoor light reaches occupants through a visual field simultaneously used for ongoing visual activity, yet ocular exposure is commonly characterized by scalar measures of magnitude and spectrum. This study examined responses to graded light exposure delivered to the temporal visual field while central task-display conditions were maintained. Thirty-three participants completed a within-subject experiment under four calibrated conditions corresponding to regional melanopic spatial doses of 0.00, 30.79, 61.58, and 92.50 lx; eye-level melanopic equivalent daylight illuminance (mEDI) was retained as a complementary scalar measure. Electrodermal activity, limited-channel EEG, cognitive performance, and subjective responses were assessed. Resting-state mean SCR amplitude was higher under all active conditions than under the near-dark reference, while prefrontal β and parietal α2 power differed mainly at the two higher exposures. All active conditions showed higher 2-back accuracy, whereas DCCS showed no significant condition effect. Visual comfort was lower at 92.50 lx and positive affect at 61.58 lx. The results show differentiated responses to spatially constrained ocular light exposure during ongoing visual activity. Regional melanopic spatial dose complements scalar mEDI by retaining spatial exposure information, although its independent contribution cannot be separated from melanopic magnitude in this design.

1. Introduction

1.1 From indoor lighting to human exposure

Much of modern work and learning takes place indoors, where people remain exposed to the surrounding light environment while reading, working at screens, and performing other visually demanding activities. As attention to indoor environmental quality has expanded toward occupants' experience and functioning, lighting has come to be considered as more than a technical requirement for visibility[1]. Ocular light exposure can also influence alertness, affect, physiological state, and cognitive functioning[2–4]. Understanding indoor lighting therefore requires attention not only to whether a space is sufficiently illuminated, but also to how the light actually received by occupants relates to human responses.

Once attention shifts from the light present in a room to the light received at the eye, the description of exposure also changes. Conventional measures such as photopic illuminance and correlated color temperature remain fundamental for evaluating visual conditions, but they capture only part of the information relevant to responses beyond vision. This recognition has supported the development of photoreceptor-weighted quantities that characterize ocular exposure according to the spectral sensitivities of the human photoreceptor system[5, 6]. Among these, melanopic equivalent daylight illuminance (mEDI) provides a standardized measure of melanopsin-weighted light at the eye and an important basis for experimental comparison and recommendations concerning daytime exposure[7, 8].

Such metrics describe exposure magnitude and spectral composition with substantially greater physiological relevance than conventional photopic quantities alone. However, ocular exposure also has a spatial organization. In occupied indoor environments, windows, luminaires, room surfaces, partitions, and the occupant's position and orientation determine where light enters the visual field[9, 10]. Source position and luminance patterns are already known to affect perceived brightness, glare, visual comfort, and impressions of an illuminated space[11, 12]. The same spatial arrangement also determines how ocular exposure is distributed across the visual field.

Scalar quantities such as mEDI remain indispensable for characterizing exposure magnitude, but they do not retain this angular organization[10, 13, 14]. Consequently, two lighting environments with similar scalar melanopic exposure may still distribute that exposure differently across the visual field. Regional-exposure studies further suggest that spatial location may be relevant to physiological and behavioral responses beyond vision, although the direction and magnitude of reported effects vary across experimental paradigms.

This evidence does not establish a fixed hierarchy of visual-field sensitivity. Rather, it identifies spatial organization as an additional property of ocular exposure. A fuller account of indoor lighting may therefore require consideration not only of how much biologically relevant light reaches the eye, but also of how that exposure is distributed across the visual field and how occupants respond under the visual conditions in which it occurs[15–18].

1.2 Regional light exposure and human responses

Experimental studies have manipulated ocular light spatially using upper–lower visual-field illumination, central and off-axis exposure, nasal and temporal retinal stimulation, and unilateral or otherwise localized light delivery[16, 18, 19]. These paradigms address different questions and are not directly interchangeable, but they share the premise that ocular light exposure has a spatial structure that can be experimentally controlled. Regional exposure has accordingly been examined in relation to melatonin suppression, pupillary regulation, alertness, and cortical electrophysiological activity, placing spatial distribution alongside exposure magnitude, spectrum, and timing as part of the conditions under which human responses are studied[17, 19, 20].

A regional label, however, does not uniquely specify the retinal stimulus. Light arriving from a portion of the visual field is transformed by ocular geometry and optics before reaching the retina. Direction of incidence is related to retinal projection and eccentricity, while source extent and illuminated area influence the spatial extent of stimulation[16, 20, 21]. These properties coexist with the photometric, spectral, and temporal characteristics of exposure. Melanopsin-containing intrinsically photosensitive retinal ganglion cells also operate within a retinal system that

integrates intrinsic melanopsin responses with rod- and cone-derived input[5, 22, 23]. Spatially resolved exposure is therefore better understood as a configuration of ocular and retinal stimulation than as a simple ranking of named visual-field regions.

The response space is similarly multidimensional. Circadian and neuroendocrine outcomes provided much of the foundational evidence that ocular light affects physiology beyond image-forming vision[5, 24], while research on acute daytime exposure has expanded to autonomic activity, cortical electrophysiology, behavioral performance, alertness, affect, effort, comfort, and environmental appraisal[2, 25–27]. These measures describe different levels of the same person–environment encounter and need not change synchronously under a given lighting condition.

The spatial dimension becomes particularly relevant during ongoing visual activity. In reading, screen-based work, and other visually demanding tasks, detailed task information is concentrated near the direction of gaze, whereas environmental illumination reaches the eye over a much wider angular field[21]. Light introduced near task-relevant content may alter local brightness and luminance contrast, while sufficiently bright or non-uniform sources can contribute to discomfort glare depending on luminance, apparent size, position, and adaptation state[11, 28, 29]. Light arriving farther from the task-dominant region may contribute less directly to the visual information required for the activity while remaining part of both ocular exposure and the visible environment.

Central and peripheral regions are not independent environments, and their boundary is neither physiologically nor perceptually absolute. What can nevertheless be controlled experimentally is the spatial relation between the region receiving additional light and the region predominantly used to acquire task information. Physiological, electrophysiological, behavioral, and subjective measurements can then be used together to characterize how the same spatially organized exposure is expressed across different response domains without treating any single measure as a proxy for the others.

1.3 Objectives of the present study

The present study examined human responses to graded ocular light exposure delivered within a controlled region of the visual field during ongoing central visual tasks. Additional light was directed to the temporal visual field while central task-display conditions were maintained. The temporal field was used as a controlled regional exposure configuration rather than as an assumed biologically privileged location, allowing the spatial relation between added ocular exposure and task-relevant visual information to be explicitly defined.

Because exposure magnitude and spatial distribution varied concurrently in the present experiment, the resulting conditions were characterized from complementary scalar and regional perspectives. Eye-level mEDI represented standardized melanopic exposure magnitude, whereas regional melanopic spatial dose retained information about the defined angular extent and organization of the exposure. These descriptors characterize different properties of the same imposed light field and do not isolate visual-field location as an independent causal factor.

Human responses were examined across psychophysiological, cognitive, and experiential domains. The study therefore addressed three related questions. First, how are acute autonomic and cortical responses associated with graded temporal visual-field exposure under stable central task-display conditions? Second, how do working-memory and cognitive-flexibility performance, together with subjective experience, vary across the same exposure conditions? Third, how are these responses expressed across multiple observational levels within a task-oriented environment in which additional ocular light is spatially separated from the central task-dominant region?

By combining controlled regional exposure with scalar and spatial melanopic characterization and multimodal human-response measurements, the study was designed to evaluate spatially constrained ocular light as an experimentally defined exposure configuration rather than to establish a privileged visual-field region, a melanopic dose threshold, or a lighting prescription.

2. Results

2.1 Exposure characterization and manipulation check

The experimental lighting configuration produced graded ocular exposure within the defined temporal visual field while maintaining the central task region under consistent viewing conditions. The active temporal-field exposure extended approximately from + 60° to + 160° in the right visual field and from − 160° to − 60° in the left visual field, whereas illuminance within the inner central task field remained below 15 lx. Background melanopic exposure from the top lighting remained below 3% of the temporal-field exposure under the active conditions. The spatial configuration and physical implementation of the temporal-field exposure are shown in Fig. 1.

Spectral composition remained stable across the three active exposure conditions.. The principal emission peaks remained at approximately 450 and 550 nm, correlated color temperature varied within ± 200 K, and normalized spectral differences across the three active conditions did not exceed 5.2%. During 30 min of continuous operation, spectral and illuminance fluctuations remained within ± 3%, indicating stable short-term output.

Melanopic daylight efficacy ratio (melanopic DER) remained nearly constant across conditions, ranging from 0.3305 to 0.3312. Using the near-dark condition as the zero reference for condition-level exposure reporting, the four conditions corresponded to eye-level mEDI values of 0.00, 231.63, 462.98, and 694.05 lx and unilateral temporal-field regional melanopic spatial doses of 0.00, 30.79, 61.58, and 92.50 lx, respectively. Left–right

differences in regional dose remained below 1.2%. These measurements confirmed a graded and reproducible temporal-field exposure while maintaining comparable spectral composition across the active conditions (Fig. 2; Table 1).

Because eye-level mEDI and regional melanopic spatial dose increased concurrently, the two exposure descriptors were strongly coupled in the present design. Regional melanopic spatial dose is therefore used below to identify the spatially constrained exposure conditions, while mEDI is retained as the corresponding scalar melanopic reference.

Table 1
Light-field characterization and melanopic exposure metrics under the four nominal temporal visual-field exposure conditions.

Nominal exposure condition	Mean Vertical Photopic Illuminance (lx)	Maximum Vertical Photopic Illuminance (lx)	Minimum Vertical Photopic Illuminance (lx)	Maximum spectral difference (%)	Eye-level mEDI (lx)	melanopic DER	Unilateral temporal-field regional melanopic spatial dose (lx)
0 lx	13.50	16.77	9.08	—	0.00	0.3312	0.00
700 lx	730.67	733.22	721.70	0.0	231.63	0.3309	30.79
1400 lx	1410.18	1415.30	1406.18	3.1	462.98	0.3307	61.58
2100 lx	2001.06	2006.82	1994.70	5.2	694.05	0.3305	92.50

Note. Nominal exposure refers to the four temporal-field illuminance settings used to define the experimental conditions. Mean, maximum, and minimum vertical photopic illuminance were derived from 36-point measurements across the diffusion panel and were used to characterize light-field uniformity. Maximum spectral difference was calculated from normalized spectral power distributions, using the nominal 700 lx condition as the active-light reference. Eye-level melanopic equivalent daylight illuminance (mEDI) and melanopic daylight efficacy ratio (melanopic DER) were derived from spectral and photometric measurements obtained with the cosine-corrected spectrometer. Unilateral temporal-field regional melanopic spatial dose was calculated for the predefined temporal visual-field region using the study-specific solid-angle-weighted spatial model and is reported in equivalent lux (lx) as a physical–spectral descriptor of regional exposure. The nominal 0-lx condition retained only very low residual background lighting and was treated as 0.00 lx on the condition-level melanopic exposure scale because this residual contribution was negligible relative to the active temporal-field exposures; 0.00 lx therefore denotes the analytical near-dark reference rather than the complete absence of optical radiation.

2.2 Subjective responses

Subjective responses differed selectively across the measured domains (Fig. 3; Supplementary Table S1). Visual comfort declined descriptively from 26.67 ± 8.72 under the near-dark reference to 26.06 ± 7.59, 25.27 ± 7.63, and 22.76 ± 8.39 under regional melanopic spatial doses of 30.79, 61.58, and 92.50 lx, respectively. Exposure condition had a significant effect on visual comfort, $F(3, 96) = 3.50$, $p = .019$, partial $\eta^2 = .098$. Bonferroni-adjusted comparisons showed lower visual comfort at 92.50 lx than under the reference condition, MD = − 3.91, 95% CI [− 7.41, − 0.41], padj = .020.

Positive affect also showed a significant condition effect, $F(3, 96) = 3.02$, $p = .033$, partial $\eta^2 = .086$. Mean positive-affect scores were 27.36 ± 6.58, 25.61 ± 7.38, 24.64 ± 8.45, and 25.30 ± 7.97 across the four dose conditions. The only significant adjusted pairwise difference was a lower positive-affect score at 61.58 lx than under the reference condition, MD = − 2.72, 95% CI [− 5.27, − 0.17], padj = .030.

Task-related workload, KSS, ESS, and negative affect showed no significant condition effects. Thus, detectable subjective differences were restricted to particular outcomes and exposure levels rather than occurring consistently across the measured experiential domains.

2.3 Cognitive task performance

Cognitive performance showed a clearer condition-related pattern for the 2-back task than for DCCS (Fig. 4; Supplementary Table S1).. Mean 2-back accuracy increased from 85.89 ± 9.85% under the near-dark reference to 91.19 ± 5.97%, 93.37 ± 6.34%, and 93.94 ± 6.25% at regional melanopic spatial doses of 30.79, 61.58, and 92.50 lx, respectively.

Exposure condition had a significant effect on 2-back accuracy, $F(3, 96) = 13.66$, $p < .001$, partial $\eta^2 = .299$. Relative to the reference condition, accuracy was higher by 5.30 percentage points at 30.79 lx, 95% CI [1.52, 9.08], padj = .002; by 7.48 percentage points at 61.58 lx, 95% CI [3.70, 11.26], padj < .001; and by 8.05 percentage points at 92.50 lx, 95% CI [4.27, 11.83], padj < .001. No adjusted differences were detected among the three active exposure conditions.

The 2-back error rate decreased descriptively under the active conditions, but the main effect was not significant, $F(3, 96) = 1.89$, $p = .136$, partial $\eta^2 = .056$.

DCCS accuracy remained high across all conditions, ranging from 96.36% to 98.59%, and neither DCCS accuracy nor error rate showed a significant condition effect, $F(3, 96) = 1.78$, $p = .155$, partial $\eta^2 = .053$. The behavioral effect was therefore concentrated in 2-back accuracy rather than being expressed consistently across both cognitive tasks.

2.4 Electrodermal responses

Electrodermal responses differed between tonic and phasic measures (Fig. 5; Supplementary Table S2). Skin conductance level showed descriptive increases under the active exposure conditions during the resting-state, 2-back, and DCCS stages, but none of the corresponding condition effects reached significance: resting-state, $F(3, 96) = 1.84$, $p = .143$, partial $\eta^2 = .041$; 2-back, $F(3, 96) = 2.01$, $p = .118$, partial $\eta^2 = .059$; and DCCS, $F(3, 96) = 2.27$, $p = .086$, partial $\eta^2 = .066$. Task-induced ΔSCL during 2-back likewise showed no condition effect, $F(3, 96) = 0.12$, $p = .947$, partial $\eta^2 = .004$.

Resting-state SCR count showed a significant omnibus condition effect, $F(3, 96) = 3.14$, $p = .028$, partial $\eta^2 = .070$, although no pairwise comparison remained significant after Bonferroni adjustment.

Resting-state mean SCR amplitude showed clearer differentiation, $F(3, 96) = 4.97$, $p = .003$, partial $\eta^2 = .104$. Relative to the near-dark reference, mean SCR amplitude was higher at 30.79 lx, MD = 5.12 μS, 95% CI [0.14, 10.10], padj = .040; at 61.58 lx, MD = 5.49 μS, 95% CI [0.51, 10.47], padj = .023; and at 92.50 lx, MD = 6.51 μS, 95% CI [1.53, 11.49], padj = .004. No significant adjusted differences were detected among the three active conditions.

Task-stage SCR count and amplitude distributions are retained descriptively in Fig. 5. Overall, the clearest electrodermal differentiation was observed in resting-state phasic response amplitude rather than tonic SCL.

2.5 EEG responses

EEG responses showed condition sensitivity for selected frequency- and site-specific measures rather than across all recorded indices (Fig. 6; Supplementary Table S3).Prefrontal β power showed significant condition effects during the resting-state, $F(3, 96) = 8.24$, $p < .001$, partial $\eta^2 = .205$; 2-back, $F(3, 96) = 7.69$, $p < .001$, partial $\eta^2 = .194$; and DCCS stages, $F(3, 96) = 7.12$, $p < .001$, partial $\eta^2 = .182$. Across all three stages, β power was lower at 61.58 and 92.50 lx than under the near-dark reference, whereas no significant difference was detected between 30.79 lx and the reference.

Parietal α2 power showed a similar cross-stage pattern. Significant condition effects were observed during the resting-state, $F(3, 96) = 9.17$, $p < .001$, partial $\eta^2 = .223$; 2-back, $F(3, 96) = 8.83$, $p < .001$, partial $\eta^2 = .216$; and DCCS stages, $F(3, 96) = 8.45$, $p < .001$, partial $\eta^2 = .209$. Across all three stages, α2 power was lower at 61.58 and 92.50 lx than under the reference condition and was also lower at 92.50 lx than at 30.79 lx.

By contrast, the prefrontal α/θ ratio showed no significant condition effect during any stage. The EEG findings therefore indicate selective modulation of prefrontal β and parietal α2 power rather than a uniform condition-related change across the selected electrophysiological indices.

3. Discussion

Across the four exposure conditions, human responses were differentiated rather than uniformly dose ordered. Spatially constrained temporal-field exposure was associated with changes in resting-state phasic electrodermal activity, selected frontal and parietal EEG measures, working-memory performance, and particular aspects of subjective experience, whereas several other outcomes showed no significant condition effects. These responses occurred while participants continued to use the central visual field for cognitive tasks and received additional ocular light within a defined region of the surrounding visual field. The findings therefore characterize responses to a spatially organized ocular exposure during active visual use rather than to an isolated full-field light stimulus. Because eye-level mEDI and regional melanopic spatial dose increased concurrently, however, the present experiment cannot distinguish the contribution of melanopic exposure magnitude from an independent effect of visual-field location.

This spatial relation is relevant because ocular light exposure in occupied environments rarely occurs independently of visual activity. During reading, screen-based work, and other task-oriented activities, visual information is concentrated near the direction of gaze while light from the surrounding environment continues to enter the eye across a broader angular field. The present experiment made this relation explicit by maintaining a stable central task display while delivering additional light to the temporal visual field. The temporal field is not interpreted here as a biologically privileged region; its experimental value lies in providing a spatially defined exposure configuration outside the central task-dominant region.

Geometric separation of the temporal-field exposure did not remove the added light from visual experience. Although central task-display luminance, contrast, viewing distance, and interface remained unchanged, the surrounding luminous environment varied across exposure conditions. Source position, luminance, apparent size, adaptation state, and spatial non-uniformity can influence how an illuminated environment is perceived[11, 28, 29]. The present paradigm should therefore be understood as controlling the spatial relationship between additional ocular exposure and central task information rather than as producing a purely non-visual stimulus.

The behavioral findings illustrate this distinction. All three active exposure conditions were associated with higher 2-back accuracy than the near-dark reference, whereas no significant differences were detected among the active conditions. DCCS performance remained high and showed no significant condition effect. The behavioral response was therefore task dependent rather than indicative of a generalized improvement in cognition with increasing exposure[26, 30, 31]. Working-memory updating may have been more sensitive to the acute lighting manipulation than the cognitive-flexibility processes assessed by DCCS, while the consistently high DCCS accuracy may have restricted the variability available for detecting condition-related differences. The present data consequently support an association between active exposure and 2-back performance, but not a monotonic dose–performance relationship or a general enhancement of cognitive functioning.

Subjective responses provide an important boundary around this behavioral pattern. Most measured subjective outcomes showed no significant condition effects, but visual comfort was lower at the highest regional dose than under the near-dark reference, and positive affect was lower at 61.58 lx in one adjusted comparison. Maintaining the central task display therefore did not imply an unchanged subjective lighting experience. The additional temporal-field light remained part of the visible scene[26, 32, 33]. Without full-field imaging luminance measurements, however, the lower visual-comfort rating at the highest exposure cannot be attributed specifically to melanopic magnitude, temporal-field position, or source luminance distribution. The finding remains environmentally meaningful because the same light that constitutes ocular exposure also forms part of the luminous scene that occupants perceive and evaluate.

Within the tested range, the 30.79-lx regional-dose condition showed a comparatively distinct empirical profile. It was the lowest active condition associated with higher 2-back accuracy and greater resting-state mean SCR amplitude than the near-dark reference, while no statistically detectable differences from the reference were observed in visual comfort or positive affect. This pattern is noteworthy, but it does not identify an optimum, threshold, or preferred exposure level. The active conditions did not differ significantly from one another in 2-back accuracy, and the present dose range was not designed to locate such a point. Measurable behavioral and phasic electrodermal differences were therefore already present at the lowest active exposure tested without the particular subjective differences observed at the higher conditions. The value of this profile lies in identifying a lower active condition worthy of further comparison, not in defining a recommended dose.

The multimodal measurements further show that different response domains should not be reduced to a single arousal or activation construct. Within the electrodermal measures, resting-state mean SCR amplitude provided the clearest pairwise differentiation, with higher values under all three active conditions than under the near-dark reference. SCR count showed an overall condition effect without significant adjusted pairwise differences, whereas tonic SCL showed no significant condition effect. These findings are more consistent with greater sensitivity of phasic electrodermal responding than with a generalized elevation of tonic skin conductance[34]. The data do not identify the retinal, central, or autonomic mechanism responsible for this pattern. Accordingly, the present pattern should not be summarized as generalized autonomic arousal.

The EEG findings were similarly selective. Prefrontal β and parietal α2 power differed across exposure conditions during the resting-state, 2-back, and DCCS stages, with the clearest contrasts occurring primarily at the two higher regional-dose conditions. By contrast, the prefrontal α/θ ratio showed no significant condition effect. The absence of a common pattern across the selected EEG indices argues against interpreting the results as a generalized shift in cortical activation. A more defensible interpretation is that the exposure conditions were associated with frequency- and site-specific differences in oscillatory activity at the recorded electrodes[4, 19].

The limited-channel EEG configuration also constrains the level of inference that can be made from these findings. Six frontal and parietal electrodes do not permit whole-brain localization, source reconstruction, network-level analysis, or attribution to a melanopsin-specific cortical pathway. Moreover, the clearest EEG differences appeared mainly at 61.58 and 92.50 lx, whereas higher 2-back accuracy was already observed at 30.79 lx. The electrophysiological and behavioral outcomes therefore did not show identical sensitivity to the exposure manipulation, and the EEG changes should not be treated as a direct neural explanation for the behavioral result[2, 26, 31].

Subjective responses likewise did not simply mirror either the physiological or behavioral measures. Visual comfort and positive affect showed condition-specific differences, whereas workload, state sleepiness, daytime dozing propensity, and negative affect did not. Electrodermal activity, cortical oscillations, cognitive performance, and subjective experience are therefore better regarded as distinct observational levels of the same person–environment interaction than as successive stages of a single physiological–behavioral pathway. The value of the multimodal design lies in identifying where response patterns converge and where they diverge.

The spatial characterization of the exposure is central to interpreting these findings. Eye-level mEDI remains a standardized and necessary descriptor of melanopically weighted exposure magnitude. As a scalar quantity, however, it does not preserve the angular arrangement from which that exposure arises[10, 13, 14]. A spatial descriptor becomes particularly useful in this context because visual-field labels alone do not specify angular extent or the physical organization of incident light[16, 18, 20]. The regional melanopic spatial dose used here was intended to retain information about the defined spatial extent and angular organization of melanopically weighted exposure within the temporal field. Its relationship with mEDI is therefore complementary rather than substitutive: mEDI characterizes standardized melanopic exposure magnitude, whereas regional spatial dose preserves information about how the defined exposure is distributed within a specified visual-field region.

This distinction remains physical and spectral rather than biological. Regional melanopic spatial dose does not represent regional ipRGC density, retinal sensitivity, functional retinal weighting, post-receptoral processing, individual pupil dynamics, ocular transmission, or gaze-dependent retinal

projection. It should therefore be interpreted as a spatial exposure descriptor rather than as a retinal or neural dose or a direct predictor of melanopsin-mediated response. Because mEDI and regional melanopic spatial dose covaried in the present experiment, the observed differences cannot be partitioned into an effect of melanopic magnitude and an independent effect of spatial organization.

The present study therefore represents a step in spatial characterization rather than spatial inference. It demonstrates that a regionally constrained ocular exposure can be physically defined, quantified, and evaluated together with multimodal human responses, but it does not establish that visual-field location independently modifies the response to an otherwise equivalent melanopic dose. Establishing such an effect requires a different comparison in which melanopic magnitude is held approximately constant while the spatial distribution of exposure is systematically reorganized across visual-field regions[16, 35]. Matched-magnitude comparisons would provide the more direct test of whether spatially resolved exposure information contributes explanatory value beyond scalar magnitude alone.

A further limitation concerns the transition from controlled geometry to occupied environments. Head stabilization and restricted viewing geometry were necessary to maintain a reproducible angular relation among the participant, central task, and temporal-field exposure. In real work and learning environments, this relation varies continuously with eye movements, head orientation, task location, and pupil size[9, 32, 36–38]. Eye tracking, concurrent pupil measurement, time-resolved light dosimetry, and full-field luminance imaging would therefore extend the present approach toward participant-specific, dynamic estimates of received light.

The present response profile is also bounded by the acute daytime exposure, young-adult sample, and limited set of centrally presented cognitive tasks. The findings do not establish effects on circadian phase, subsequent sleep, repeated daily exposure, chronic health outcomes, other age groups, or activities with different visual demands. The EDA, EEG, behavioral, and subjective measures examined here are also not pathway-specific biomarkers of melanopsin activity. Future work should therefore combine controlled matched-magnitude spatial comparisons with more naturalistic studies of how ocular exposure changes as occupants move and interact with spatially complex indoor environments. In everyday indoor settings, magnitude, spectrum, spatial distribution, and visual activity are analytically separable but experienced simultaneously[9, 10, 39].

Taken together, the present experiment does not establish a privileged visual-field region or an independent spatial biological effect, but it provides a controlled framework for characterizing spatially constrained melanopic exposure and examining how that exposure is expressed across multiple human-response domains during ongoing visual activity. The next decisive question is whether exposures matched in melanopic magnitude remain equivalent when the same light is reorganized across different portions of the visual field.

4. Conclusion

This study shows that spatially constrained temporal-field light exposure can be experimentally defined, quantified, and associated with differentiated physiological, electrophysiological, cognitive, and subjective responses during ongoing central visual tasks. Regional melanopic spatial dose provides a complementary descriptor of the angular organization of melanopically weighted exposure alongside scalar eye-level mEDI.

The present findings do not establish an independent effect of visual-field location, a privileged temporal-field region, or an optimal exposure level, because melanopic magnitude and regional spatial dose varied concurrently. Future studies should therefore compare lighting conditions matched in melanopic magnitude but redistributed across different visual-field regions to determine whether spatial organization contributes explanatory value beyond scalar exposure alone.

5. Methods

5.1 Participants, ethics, and study design

The study protocol was reviewed and approved by the Scientific and Technological Ethics Committee of Northeast Forestry University (approval no. [2026128]; approval date: [15 January 2026]). All participants provided written informed consent prior to participation. All procedures involving human participants were conducted in accordance with the Declaration of Helsinki and the relevant institutional guidelines and regulations.

The study was designed as a controlled, within-subject repeated-measures laboratory experiment in healthy adults to characterize acute human responses to graded environmental light exposure and was not conducted as a clinical trial. Forty-five university students aged 18–30 years were initially recruited. Sample size was determined with reference to comparable laboratory studies of acute light exposure; no formal a priori power analysis was conducted[17, 26]. Eligibility criteria included normal or corrected-to-normal vision, absence of color blindness, no self-reported psychiatric, neurological, or sleep disorders, no use of centrally acting medications during the preceding 6 months, and no long-term contact-lens use. Nine participants withdrew from the study, two were excluded because of missing physiological data, and one was excluded because of invalid questionnaire data. The final analytic sample therefore comprised 33 participants (18 men and 15 women; mean age = 24.46 years, SD = 1.80).

Each participant completed four temporal visual-field exposure conditions with nominal illuminance settings of 0, 700, 1400, and 2100 lx. The nominal 0-lx condition served as a near-dark reference condition and retained only low-level background top lighting. Condition order was assigned using a randomized Latin-square design to reduce systematic order effects, and successive sessions for the same participant were separated by at least one week.

All experimental sessions began at 14:00 local time. Thus, the four sessions completed by each participant were conducted at the same time of day to reduce variation associated with time-dependent physiological and cognitive responses. Sessions for female participants were scheduled outside self-reported menstruation; menstrual-cycle phase was not otherwise assessed or controlled.

5.2 Laboratory environment and temporal visual-field lighting configuration

Experiments were conducted in a fully enclosed lighting laboratory without daylight exposure. The laboratory measured 9.89 × 7.85 × 3.15 m. Participant position, viewing direction, and the angular relationship between the eye and the lighting system were fixed throughout testing. A forehead rest was used to stabilize head position, and eye height was maintained at approximately 1.20 m.

Temporal-field illumination was physically separated from the central task-dominant field using left and right blackout panels. The panel boundaries were positioned at approximately − 60° and + 60° relative to the central visual axis, with a calibration tolerance of ± 1.5°. This arrangement shielded the central 120° horizontal sector from direct temporal-field illumination. The resulting active exposure extended approximately from + 60° to + 160° in the right visual field and from − 160° to − 60° in the left visual field, with a vertical extent of approximately − 70° to + 70° relative to the central visual axis.

A symmetrical 3 × 3 LED array was installed on each side of the participant. Each LED was rated at 35 W and had a nominal beam angle of 40°. The distance from each LED array to the participant was approximately 1.8 m. A diffusion panel measuring approximately 2.0 × 1.3 m, with a nominal transmittance of at least 90%, was positioned between each lighting array and the participant to improve regional field uniformity and reduce localized differences in source luminance.

The spectral composition of the temporal-field lighting was maintained across the active exposure conditions, whereas nominal temporal-field illuminance was varied across the four experimental levels. The nominal 0-lx condition served as the near-dark reference and retained only very low background top lighting. This residual background contribution was negligible relative to the active temporal-field exposures and was therefore taken as the zero reference for condition-level melanopic exposure reporting. Accordingly, 0.00 lx denotes the analytical near-dark reference of the experimental exposure scale rather than the complete absence of optical radiation.

Within the inner central task field, defined operationally as approximately − 30° to + 30° around the visual axis, illuminance remained below 15 lx under the active temporal-field exposure conditions. Background melanopic exposure attributable to the top lighting was maintained below 3% of the temporal-field exposure under the active conditions. These controls were intended to concentrate the experimental manipulation outside the task-dominant central field while maintaining the central visual-task configuration.

The central task display was positioned 90 cm from the participant. Display luminance was maintained at 200 cd/m² and the contrast ratio at 800:1. Display settings, task interface, viewing distance, and participant position were kept unchanged across the four exposure conditions. The display was used exclusively to present the centrally located cognitive tasks and was not manipulated as part of the temporal-field lighting intervention.

Additional monitors visible behind the participant in photographs of the experimental setup formed part of the physiological-signal acquisition and experiment-monitoring workstation. They were used for EEG and electrodermal data acquisition, task synchronization, and real-time monitoring of task presentation. Participants faced away from these monitors throughout testing, and the monitors remained outside the participant's visual field. Their configuration and operating state were kept constant across exposure conditions.

5.3 Light-field measurement and optical characterization

Optical measurements were conducted at the participant's eye position using an ATP6520 cooled spectrometer (OPTOSKY, Xiamen, China) equipped with a 180° cosine corrector. Spectral power distribution (SPD) was measured under each of the four exposure conditions. Twenty-four repeated SPD measurements were obtained for each condition, with dark-current correction applied to the measurements.

Spatial uniformity of the temporal-field illumination was additionally evaluated by measuring vertical photopic illuminance at 36 locations distributed across the diffusion panel. To assess temporal stability, the lighting system was operated continuously for 30 min at each exposure level while spectral and illuminance measurements were repeated. These procedures provided complementary assessments of spectral reproducibility, regional uniformity, and temporal stability.

An imaging luminance meter was not used in the present experiment; consequently, the luminance distribution of the complete visual scene was not directly quantified. Optical verification instead combined eye-level spectral measurements, vertical photopic illuminance measurements, melanopic quantities, regional spatial-dose characterization, and repeated temporal-stability measurements. The implications of the absence of full-field imaging luminance measurements are considered when interpreting the visual-comfort findings.

Measured vertical photopic illuminance was retained as a calibration and light-field verification quantity. Melanopic equivalent daylight illuminance (mEDI) was used as the standardized scalar descriptor of melanopically weighted ocular exposure, whereas regional melanopic spatial dose was used to retain information about the defined angular distribution of the temporal-field exposure.

5.4 Melanopic exposure and regional melanopic spatial-dose calculation

Melanopic quantities were calculated according to the CIE S 026/E:2018 α-opic photometry framework[7]. In the calculation implemented in the present study, melanopic irradiance was obtained from the measured spectral power distribution (SPD) and the melanopic spectral weighting function:

$$\varvec{E}_{\varvec{e},\mathbf{mel}} = \int_{380}^{780} \varvec{E}_{\varvec{e},\varvec{\lambda}}\left(\varvec{\lambda}\right)\varvec{s}_{\mathbf{mel}}\left(\varvec{\lambda}\right)\varvec{d}\varvec{\lambda}$$

where $E_{e,\lambda}\left(\lambda\right)$ represents the measured spectral irradiance and $s_{\mathrm{mel}}\left(\lambda\right)$ represents the melanopic spectral weighting function.

Melanopic equivalent daylight illuminance (mEDI) was then calculated as:

$$\varvec{E}_{\varvec{v},\mathbf{mel}}^{\varvec{D65}} = \frac{\varvec{E}_{\varvec{e},\mathbf{mel}}}{\varvec{K}_{\mathbf{mel},\varvec{v}}^{\varvec{D65}}}$$

where $K_{\mathrm{mel},v}^{D65}$ is the fixed melanopic efficacy of luminous radiation for CIE standard daylight D65. The melanopic daylight efficacy ratio (melanopic DER) was expressed as:

$$\varvec{\gamma}_{\mathbf{mel},\varvec{v}}^{\varvec{D65}} = \frac{\varvec{E}_{\varvec{v},\mathbf{mel}}^{\varvec{D65}}}{\varvec{E}_{\varvec{v}}} = \frac{\varvec{K}_{\mathbf{mel},\varvec{v}}}{\varvec{K}_{\mathbf{mel},\varvec{v}}^{\varvec{D65}}}$$

where E_v denotes photopic illuminance. Melanopic EDI is expressed in lux, whereas melanopic DER is dimensionless.

Eye-level mEDI characterizes melanopically weighted exposure as a scalar quantity and therefore does not retain the angular structure of a spatially non-uniform exposure. A regional melanopic spatial-dose calculation was consequently used to describe the imposed temporal-field configuration. The effective temporal visual field was discretized into 5° × 5° angular units, and the melanopically weighted contribution assigned to each unit in the spatial model was combined using solid-angle-based geometric weighting. Unilateral temporal-field regional melanopic spatial dose was represented as:

$$\varvec{D}_{\varvec{m}\varvec{e}\varvec{l},\varvec{r}\varvec{e}\varvec{g}} = \sum_{\varvec{i}\in\varvec{R}} \varvec{E}_{\varvec{v},\varvec{m}\varvec{e}\varvec{l},\varvec{i}}^{\varvec{D65}}\varvec{w}_{\varvec{i}}$$

where R denotes the predefined unilateral temporal-field region, $E_{v,\mathrm{mel},i}^{D65}$ denotes the melanopically weighted exposure contribution assigned to angular unit i in the implemented spatial model, and w_i denotes the solid-angle-based geometric weight assigned to that unit. The underlying solid-angle contribution of each angular unit was obtained in spherical coordinates as:

$$\varvec{\Delta\Omega}_{\varvec{i}} = \mathbf{sin}\left(\varvec{\theta}_{\varvec{i}}\right)\varvec{\Delta\theta}\,\varvec{\Delta\phi}$$

where θ_i denotes the polar angle used in the spherical-coordinate implementation, and $\Delta\theta$ and $\Delta\phi$ denote the angular increments of the grid. Both angular increments corresponded to 5° and were converted to radians for numerical calculation.

The resulting unilateral temporal-field regional melanopic spatial dose was reported in equivalent lux (lx) and used as a study-specific physical-spectral descriptor of the imposed regional exposure. It preserves information about the extent and angular organization of melanopically weighted light within the predefined temporal field that is not retained by a single eye-level scalar value and is therefore complementary to, rather than a substitute for, mEDI.

Importantly, the regional metric does not represent a biological weighting function for individual retinal regions. The solid-angle-based spatial weighting does not encode regional ipRGC density, photoreceptor sensitivity, functional retinal weighting, or post-receptoral neural processing. The calculation also does not incorporate participant-specific pupil dynamics, ocular transmission, or gaze-dependent retinal projection. Regional melanopic spatial dose should therefore be interpreted as a descriptor of the physical and spectral organization of ocular exposure rather than as a retinal neural dose or a direct predictor of melanopsin-mediated response.

For condition-level presentation of the human-response data, the nominal near-dark reference was treated as the zero point of the experimental exposure scale. The corresponding unilateral temporal-field regional melanopic spatial doses were therefore 0.00, 30.79, 61.58, and 92.50 lx, while eye-level mEDI values were 0.00, 231.63, 462.98, and 694.05 lx. Eye-level mEDI was retained in parallel as the scalar melanopic exposure reference. The complete manipulation-check results, including spectral and temporal stability and the correspondence between nominal illuminance, measured photopic illuminance, mEDI, and regional spatial dose, are reported in the Results.

5.5 Experimental procedure and cognitive tasks

Participants were instructed to abstain from alcohol, caffeine, and strong tea during the week preceding each experimental session and to obtain at least 7 h of sleep per night. Participants were also asked to arrive with clean, dry hair to facilitate stable EEG electrode contact.

Each experimental session lasted approximately 25 min following preparation of the physiological recording equipment. Participant head position was stabilized using the forehead rest throughout exposure and task performance, and viewing distance to the central display was maintained at 90 cm.

After 10 min of adaptation to the assigned lighting condition, 5 min of resting-state physiological activity was recorded. Participants then completed two centrally presented, screen-based cognitive tasks under the same lighting condition. A 2-back task was used to assess working-memory updating, and a Dimensional Change Card Sort (DCCS) task was used to assess cognitive flexibility and rule switching[40, 41]. The same task presentation, display settings, viewing geometry, and response procedures were used during all four exposure sessions.

After completion of the cognitive tasks, participants completed the subjective measures described below. Lighting exposure remained assigned according to the experimental condition throughout the corresponding session.

For behavioral analysis, task performance was represented by accuracy and error-rate measures for both the 2-back and DCCS tasks. Missed responses in the 2-back task were recorded separately from incorrect responses; consequently, the reported 2-back error rate represents incorrect responses rather than the combined proportion of incorrect and missed trials.

5.6 Subjective measures

Subjective assessment covered current sleepiness, daytime dozing propensity, positive and negative affect, visual comfort, and perceived task-related workload. All questionnaires were administered in Chinese. Complete copies of the Chinese-language forms used during the experiment and author-prepared English translations are provided in the Supplementary Information. The English versions were prepared for reporting transparency and were not administered to participants.

Current subjective sleepiness was assessed using the single-item Karolinska Sleepiness Scale[42]. Participants selected one of nine levels ranging from 1 to 9, with higher scores representing greater current sleepiness.

Daytime dozing propensity was assessed using the eight-item Epworth Sleepiness Scale. Each of eight everyday situations was rated from 0 to 3 according to the likelihood of dozing[43]. Item scores were summed to provide a total score ranging from 0 to 24, with higher scores representing a greater propensity to doze in everyday situations.

Positive and negative affect were assessed using a 20-item PANAS-based questionnaire adapted to the experimental task context[44]. The measure contained 10 positive-affect items and 10 negative-affect items. Each item was rated on a five-point response scale with reference to the participant's experience during the just-completed experimental period. Positive-affect (PA) and negative-affect (NA) items were summed separately, producing subscale scores ranging from 10 to 50. Higher scores represented stronger positive or negative affect, respectively. Because the wording was adapted for the present task context, the measure is treated here as PANAS-based rather than as an unmodified administration of the original PANAS.

Visual comfort was evaluated using a study-specific eight-item questionnaire. Items addressed ocular comfort, visual fatigue, perceived lighting uniformity, perceived appropriateness of brightness, ease of concentration, headache or physical discomfort attributable to the lighting, ease of reading or observing objects, and overall satisfaction with the lighting environment. Each item was rated from 1 to 5, and the eight responses were summed to produce a total score ranging from 8 to 40. Higher scores represented greater visual comfort.

Task-related workload was evaluated using a study-specific six-item questionnaire comprising three two-item dimensions: time pressure, effort, and task difficulty. Items were rated on a five-point scale. Items 1, 4, and 5 were reverse-scored before aggregation so that all items were directionally aligned. The six aligned item scores were summed to provide a total workload score ranging from 6 to 30, with higher scores representing greater perceived workload.

5.7 EEG and electrodermal acquisition

EEG activity was recorded using a REEG64 system (Zhongke Zhiying, Beijing, China) at a sampling rate of 1200 Hz. Six scalp channels were recorded: FP1, FP2, F3, F4, P3, and P4. Mastoid electrodes were used as references, and electrode impedance was maintained at ≤ 5 kΩ during recording. The primary EEG outcomes reported in the present study were derived from the frontal-polar FP1/FP2 and parietal P3/P4 channels. F3/F4 were recorded as part of the limited-channel montage but were not used to construct the primary regional EEG indices reported here.

Electrodermal activity was recorded using an ErgoLAB EXG system (Kingfar, Beijing, China) at 128 Hz. Electrodes were attached to the index and middle fingers of the participant's non-dominant hand. Electrodermal recording continued across the resting-state, 2-back, and DCCS stages, allowing tonic and phasic activity to be characterized separately for the predefined experimental periods.

5.8 Signal processing and outcome derivation

All signal processing and statistical analyses were performed using MATLAB R2024b (MathWorks, Natick, MA, USA). EEGLAB was used for EEG processing, and Ledalab was used for electrodermal decomposition[45].

EEG preprocessing included electrode-location assignment, re-referencing, high-pass filtering at 0.1 Hz, low-pass filtering at 100 Hz, 50-Hz notch filtering, downsampling, and independent component analysis (ICA). Components associated with ocular artifacts were identified using automated marking together with visual inspection and were manually removed before spectral analysis.

Power spectral density was estimated using Welch's method[46]. The frequency ranges used in the present analyses were θ = 4–8 Hz, α = 8–13 Hz, α2 = 10–13 Hz, and β = 13–30 Hz. Prefrontal β power and the prefrontal α/θ ratio were calculated from FP1 and FP2 and averaged across the two channels, whereas parietal α2 power was calculated from P3 and P4 and averaged across the two parietal channels. EEG power measures were expressed in μV^2, whereas the α/θ ratio was dimensionless. EEG outcomes were calculated separately for the resting-state, 2-back, and DCCS stages.

Electrodermal recordings were low-pass filtered at 1 Hz and decomposed into tonic and phasic components using Continuous Decomposition Analysis (CDA) in Ledalab[47]. Phasic skin conductance responses exceeding a minimum amplitude criterion of 0.05 μS were automatically detected. Skin conductance level (SCL) was used to characterize tonic electrodermal activity. SCR count was defined as the number of automatically detected phasic skin conductance responses within each predefined experimental stage, and mean SCR amplitude was calculated as the mean amplitude of the detected responses within that stage[34].

SCL was derived separately for the resting-state, 2-back, and DCCS periods. For the 2-back stage, task-induced ΔSCL was calculated as the task-period SCL minus the immediately preceding resting-state SCL. Resting-state SCR count and mean SCR amplitude were included in the inferential analyses. Task-stage SCR count and SCR-amplitude distributions were retained as descriptive measures rather than being included in the corresponding inferential summary.

Questionnaire totals were calculated according to the scoring procedures described above. Cognitive outcomes were calculated separately for the 2-back and DCCS tasks, and physiological, cognitive, and subjective measures were retained as distinct response domains rather than being combined into a single composite endpoint.

5.9 Statistical analysis

The normality of model residuals was assessed using Lilliefors tests together with visual inspection of Q–Q plots. Exposure condition was treated as a four-level within-subject factor. One-way repeated-measures analyses of variance were conducted separately for the subjective, cognitive, electrodermal, and EEG outcomes.

For physiological outcomes measured during multiple experimental stages, the corresponding stage-specific variables were analyzed separately. Sphericity was evaluated using Mauchly's test. When the assumption of sphericity was violated, Greenhouse–Geisser correction was applied to the relevant test.

Partial eta squared (partial η^2) was reported as the effect-size measure for omnibus repeated-measures effects. When an omnibus effect of exposure condition was statistically significant, Bonferroni-adjusted pairwise comparisons were performed. Pairwise results were characterized using mean differences, 95% confidence intervals, and adjusted p values. Statistical significance was defined as $p < .05$.

Declarations

Competing Interests

The authors declare no competing interests.

Author Contribution

Y.H. contributed to conceptualization, data curation, formal analysis, investigation, methodology, software, visualization, and writing of the original draft, and participated in reviewing and editing the manuscript. B.L. contributed to conceptualization, methodology, supervision, and writing, reviewing, and editing the manuscript. Y.D. contributed to investigation, software, visualization, and reviewing and editing the manuscript. L.Y. contributed to methodology and reviewing and editing the manuscript. All authors reviewed and approved the final manuscript.

Acknowledgements

This research did not receive any specific grant from funding agencies in the public, commercial, or not-for-profit sectors.

Data Availability

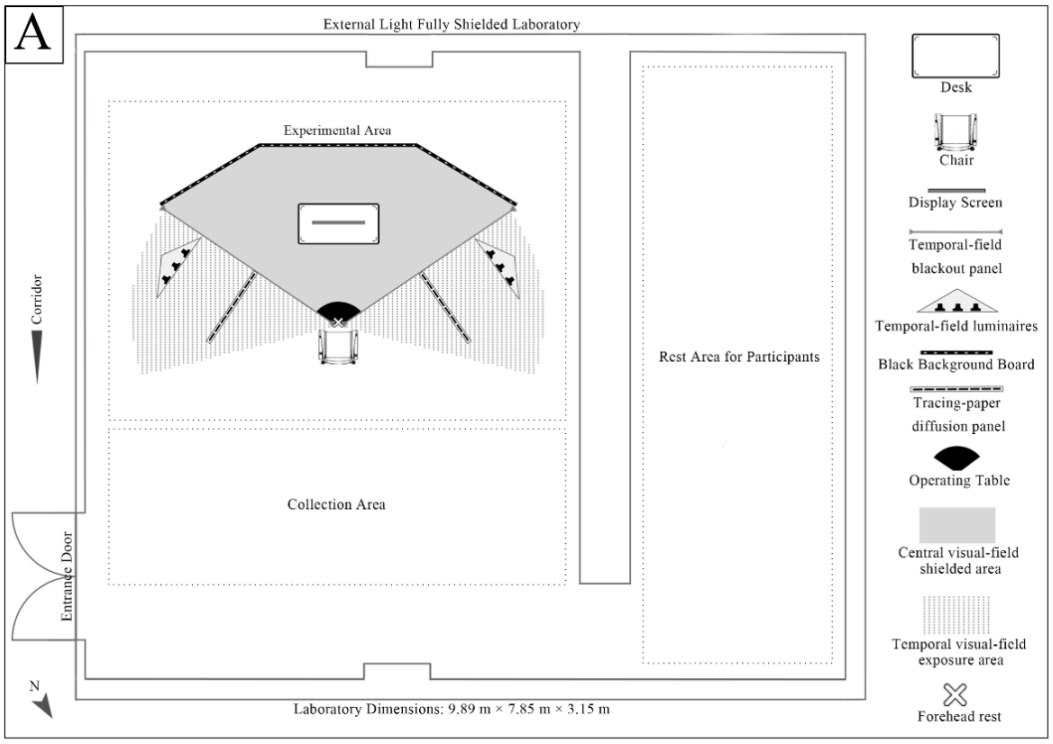
The data that support the findings of this study are available from the corresponding author upon reasonable request.

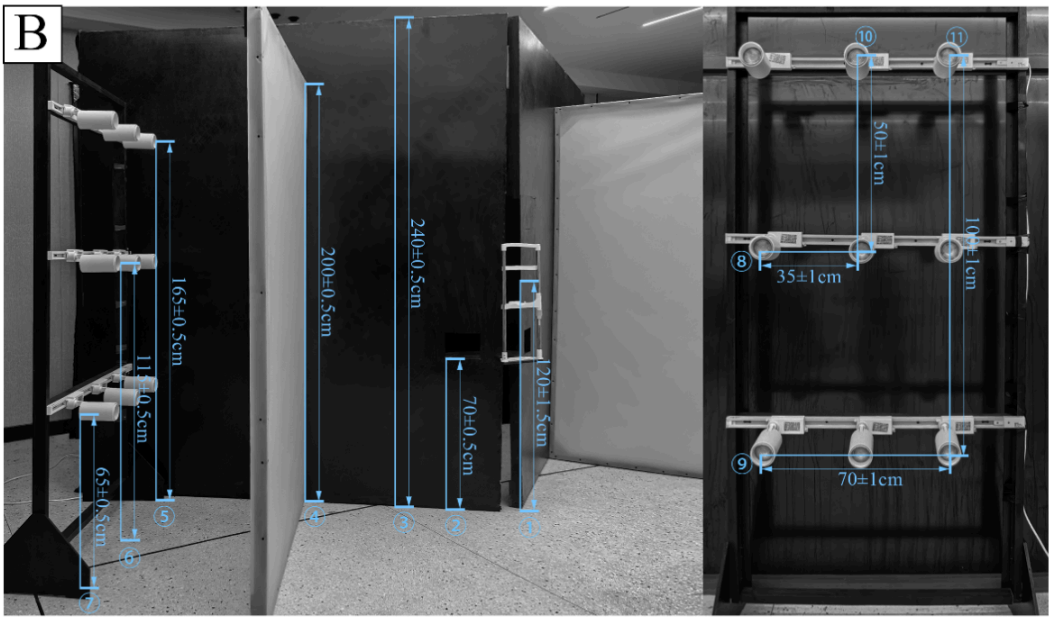
References

1. Nunayon, S. S. & Zhong, L. A mixed-method systematic review of indoor environmental quality (IEQ) gaps and opportunities for future research. *Sustain. Cities Soc.* **130**, 106535 (2025).
2. Vetter, C. et al. A review of human physiological responses to light: implications for the development of integrative lighting solutions. *Leukos* **18**, 387–414 (2022).
3. Cajochen, C. Alerting effects of light. *SLEEP. Med. Rev.* **11**, 453–464 (2007).
4. Lockley, S. W., Evans, E. E., Scheer, F. A. J. L. & Brainard, G. C. Short-wavelength sensitivity for the direct effects of light on alertness, vigilance, and the waking electroencephalogram in humans. *Sleep* 1–8. 10.1093/sleep/29.2.161 (2006).
5. Lucas, R. J. et al. Measuring and using light in the melanopsin age. *Trends Neurosci.* **37**, 1–9 (2014).
6. Schlangen, L. J. M. & Price, L. L. A. The lighting environment, its metrology, and non-visual responses. *Front. Neurol.* **12**, 624861 (2021).
7. CIE. CIE S 026/E. :2018 system for metrology of optical radiation for ipRGC-influenced responses. *Int. Comm. Illum*. https://doi.org/10.25039/S026.2018 (2018).
8. Brown, T. M. et al. Recommendations for daytime, evening, and nighttime indoor light exposure to best support physiology, sleep, and wakefulness in healthy adults. *PLOS Biol.* **20**, e3001571 (2022).
9. Amundadottir, M. L., Rockcastle, S., Sarey Khanie, M. & Andersen, M. A human-centric approach to assess daylight in buildings for non-visual health potential, visual interest and gaze behavior. *Build. Environ.* **113**, 5–21 (2017).
10. Hartmeyer, S. L., Rudawski, F. R., Knoop, M. & Andersen, M. Exploring spatiotemporal dynamics in light-dosimetry. *J. Phys. Conf. Ser.* **2600**, 112005 (2023).
11. Geerdinck, L. M., Van Gheluwe, J. R. & Vissenberg, M. C. J. M. Discomfort glare perception of non-uniform light sources in an office setting. *J. Environ. Psychol.* **39**, 5–13 (2014).
12. Loe, L., Mansfield, K. P. & Rowlands, E. Appearance of lit environment and its relevance in lighting design: Experimental study. *Light Res. Technol.* **26**, 119–133 (1994).
13. Hartmeyer, S. & Andersen, M. Towards a framework for light-dosimetry studies: quantification metrics. *Light Res. Technol.* **56**, 337–365 (2022).
14. Spitschan, M. et al. Ocular light and optical radiation exposure as a modifiable environmental determinant of health: expert consensus on research gaps and priorities. *BMC Med.* **24**, 119 (2026).
15. Glickman, G. et al. Inferior retinal light exposure is more effective than superior retinal exposure in suppressing melatonin in humans. *J. Biol. Rhythms*. **18**, 71–79 (2003).
16. Nagare, R., Rea, M. S. & Figueiro, M. G. Spatial sensitivity of human circadian response: melatonin suppression from on-axis and off-axis light exposures. *Neurobiol. SLEEP. Circadian Rhythms*. **11**, 100071 (2021).
17. Derengowski, N., Knoop, M. & Völker, S. The effect of light directionality on alertness and cognitive performance during post-lunch dip. *Light Res. Technol.* **57**, 28–46 (2025).
18. Rüger, M., Gordijn, M. C. M., Beersma, D. G. M., De Vries, B. & Daan, S. Nasal versus temporal illumination of the human retina: effects on core body temperature, melatonin, and circadian phase. *J. Biol. Rhythms*. **20**, 60–70 (2005).
19. Cajochen, C., Biase, R. D. & Imai, M. Interhemispheric EEG asymmetries during unilateral bright-light exposure and subsequent sleep in humans. *Am. J. Physiol. -Regul Integr. Comp. Physiol.* **294**, R1053–R1060 (2008).
20. Kubota, N., Tamori, Y., Baba, K. & Yamanaka, Y. Effects of different light incident angles via a head-mounted device on the magnitude of nocturnal melatonin suppression in healthy young subjects. *Sleep. Biol. Rhythms*. **20**, 247–254 (2022).
21. Curcio, C. A., Sloan, K. R., Kalina, R. E. & Hendrickson, A. E. Human photoreceptor topography. *J. Comp. Neurol.* **292**, 497–523 (1990).
22. Do, M. T. H. & Yau, K. W. Intrinsically photosensitive retinal ganglion cells. *Physiol. Rev.* **90**, 1547–1581 (2010).
23. Dacey, D. M. et al. Melanopsin-expressing ganglion cells in primate retina signal colour and irradiance and project to the LGN. *Nature* **433**, 749–754 (2005).
24. Brainard, G. C. et al. Action spectrum for melatonin regulation in humans: evidence for a novel circadian photoreceptor. *J. Neurosci.* **21**, 6405–6412 (2001).
25. Spitschan, M. Melanopsin contributions to non-visual and visual function. *Curr. Opin. Behav. Sci.* **30**, 67–72 (2019).
26. Zeng, Y. et al. The effects of lighting levels on the perception, performance and physiological responses in offices. *J. Environ. Psychol.* **107**, 102804 (2025).

27. Vandewalle, G. et al. Wavelength-dependent modulation of brain responses to a working memory task by daytime light exposure. *Cereb. Cortex*. **17**, 2788–2795 (2007).
28. Quek, G. et al. Comparing performance of discomfort glare metrics in high and low adaptation levels. *Build. Environ.* **206**, 108335 (2021).
29. Bargary, G., Jia, Y. & Barbur, J. L. Mechanisms for Discomfort Glare in Central Vision. *Invest. Ophthalmol. Vis. Sci.* **56**, 464–471 (2015).
30. Mu, Y. M. et al. Alerting effects of light in healthy individuals: a systematic review and meta-analysis. *Neural Regen Res.* **17**, 1929 (2022).
31. Smolders, K. C. H. J. & De Kort, Y. A. W. Bright light and mental fatigue: effects on alertness, vitality, performance and physiological arousal. *J. Environ. Psychol.* **39**, 77–91 (2014).
32. Peeters, S. T., Smolders, K. C. H. J., Vogels, I. M. L. C. & De Kort, Y. A. W. Less is more? Effects of more vs. less electric light on alertness, mood, sleep and appraisals of light in an operational office. *J. Environ. Psychol.* **74**, 101583 (2021).
33. Chamilothori, K., Wienold, J., Moscoso, C., Matusiak, B. & Andersen, M. Subjective and physiological responses towards daylit spaces with contemporary façade patterns in virtual reality: Influence of sky type, space function, and latitude. *J. Environ. Psychol.* **82**, 101839 (2022).
34. Society For Psychophysiological Research Ad Hoc Committee On Electrodermal Measures. Publication recommendations for electrodermal measurements. *Psychophysiology* **49**, 1017–1034 (2012).
35. Derengowski, N., Knoop, M. & Völker, S. A controlled lab experiment on the effect of light exposure of different source sizes on subjective alertness and cognitive performance during the post-lunch dip. *Light Res. Technol.* **58**, 107–122 (2026).
36. De Vries, S., Gkaintatzi-Masouti, M., Van Duijnhoven, J., Mardaljevic, J. & Aarts, M. Recommendations for light-dosimetry field studies based on a meta-analysis of personal light levels of office workers. *Light Res. Technol.* **57**, 47–70 (2025).
37. Salamone, F. et al. Wearable monitoring for evaluating non-visual effects of light on health and well-being: a systematic review. *Build. Environ.* **284**, 113482 (2025).
38. Peeters, S. T., Smolders, K. C. H. J. & De Kort, Y. A. W. What you set is (not) what you get: how a light intervention in the field translates to personal light exposure. *Build. Environ.* **185**, 107288 (2020).
39. Biller, A. M., Balakrishnan, P. & Spitschan, M. Behavioural determinants of physiologically-relevant light exposure. *Commun. Psychol.* **2**, 114–124 (2024).
40. Kirchner, W. K. Age differences in short-term retention of rapidly changing information. *J. Exp. Psychol.* **55**, 352–358 (1958).
41. Zelazo, P. D. The dimensional change card sort (DCCS): a method of assessing executive function in children. *Nat. Protoc.* **1**, 297–301 (2006).
42. Åkerstedt, T. & Gillberg, M. Subjective and objective sleepiness in the active individual. *Int. J. Neurosci.* **52**, 29–37 (1990).
43. Johns, M. W. A new method for measuring daytime sleepiness: the epworth sleepiness scale. *Sleep* **14**, 540–545 (1991).
44. Watson, D., Clark, L. A. & Tellegen, A. Development and validation of brief measures of positive and negative affect: the PANAS scales. *J. Pers. Soc. Psychol.* **54**, 1063–1070 (1988).
45. Delorme, A. & Makeig, S. EEGLAB: an open source toolbox for analysis of single-trial EEG dynamics including independent component analysis. *J. Neurosci. Methods*. **134**, 9–21 (2004).
46. Welch, P. The use of fast fourier transform for the estimation of power spectra: a method based on time averaging over short, modified periodograms. *IEEE Trans. Audio Electroacoustics*. **15**, 70–73 (1967).
47. Benedek, M. & Kaernbach, C. A continuous measure of phasic electrodermal activity. *J. Neurosci. Methods*. **190**, 80–91 (2010).

Figures





① Eye level above floor
② Operating platform height from ground level
③ Height of the temporal side barrier
④ Height of the tracing-paper diffusion panel
⑤ Height of the upper row of lights above the ground
⑥ Height of the middle row lights above the ground
⑦ Height of the lower row of lights above the ground
⑧ Horizontal spacing between adjacent luminaires
⑨ Horizontal spacing between the outermost luminaires
⑩ Vertical spacing between adjacent luminaires
⑪ Vertical spacing between outermost luminaires

Figure 1

Experimental environment and temporal visual-field exposure configuration.(A) Plan view of the fully shielded laboratory showing the experimental area, participant position, central task display, temporal-field blackout panels, luminaires, diffusion panels, central visual-field shielded area, and temporal visual-field exposure regions. (B) Photographs of the temporal-field lighting apparatus and the principal geometric dimensions used to define the experimental configuration. Numbered annotations indicate eye height, platform and panel heights, luminaire heights, and horizontal and vertical luminaire spacing.

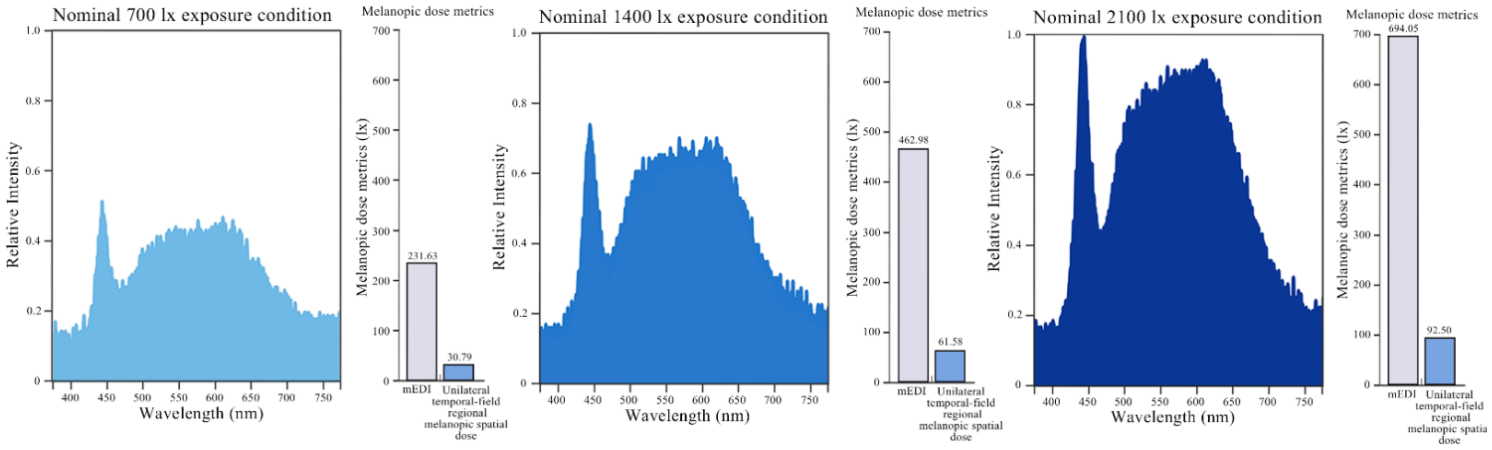


Figure 2

Spectral and melanopic characterization of the three active temporal-field exposure conditions.

Normalized spectral power distributions are shown for the nominal 700, 1400, and 2100 lx conditions together with the corresponding eye-level melanopic equivalent daylight illuminance (mEDI) and unilateral temporal-field regional melanopic spatial dose. The spectral profiles retained similar overall shapes across the active conditions while melanopic exposure magnitude increased progressively.

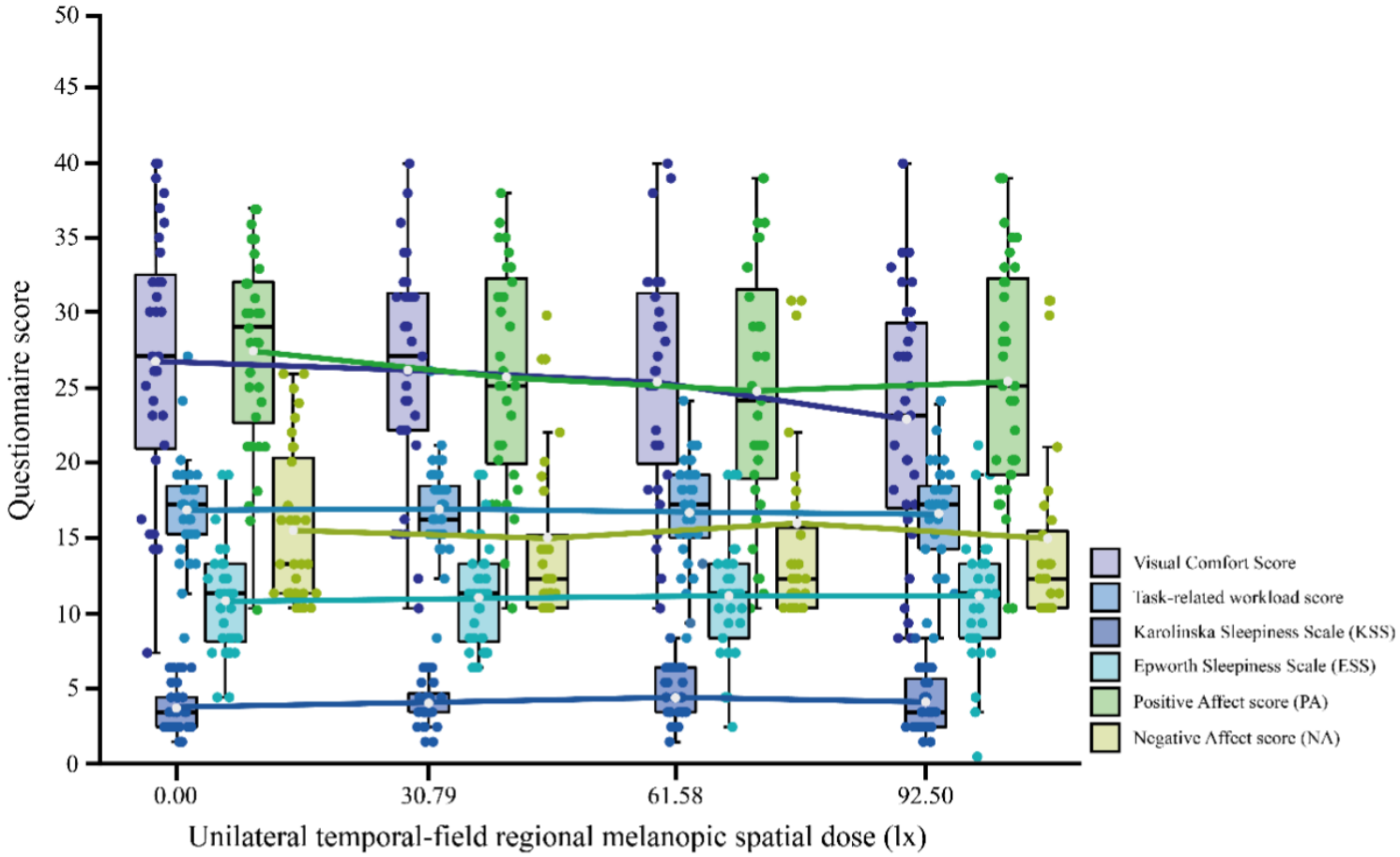


Figure 3

Subjective responses across the four regional melanopic spatial-dose conditions.Distributions of visual comfort, task-related workload, Karolinska Sleepiness Scale (KSS), Epworth Sleepiness Scale (ESS), positive affect (PA), and negative affect (NA) scores are shown for regional melanopic spatial doses of 0.00, 30.79, 61.58, and 92.50 lx. Individual observations and distribution summaries are displayed for each exposure condition.

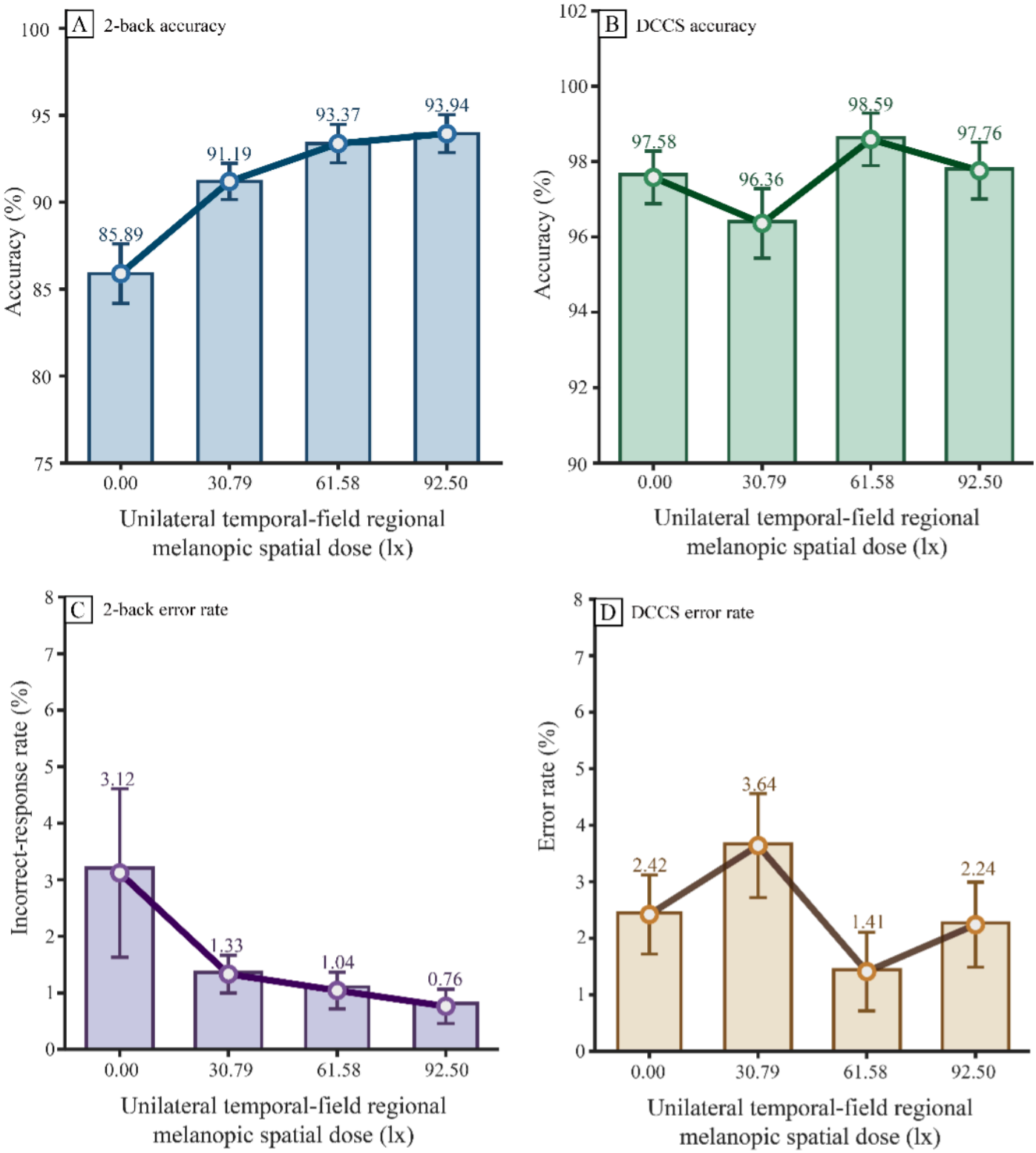


Figure 4

Cognitive task performance across the four regional melanopic spatial-dose conditions.(A) 2-back accuracy, (B) DCCS accuracy, (C) 2-back error rate, and (D) DCCS error rate under regional melanopic spatial doses of 0.00, 30.79, 61.58, and 92.50 lx. Points and error bars show condition-level summary estimates and their variability. DCCS, Dimensional Change Card Sort.

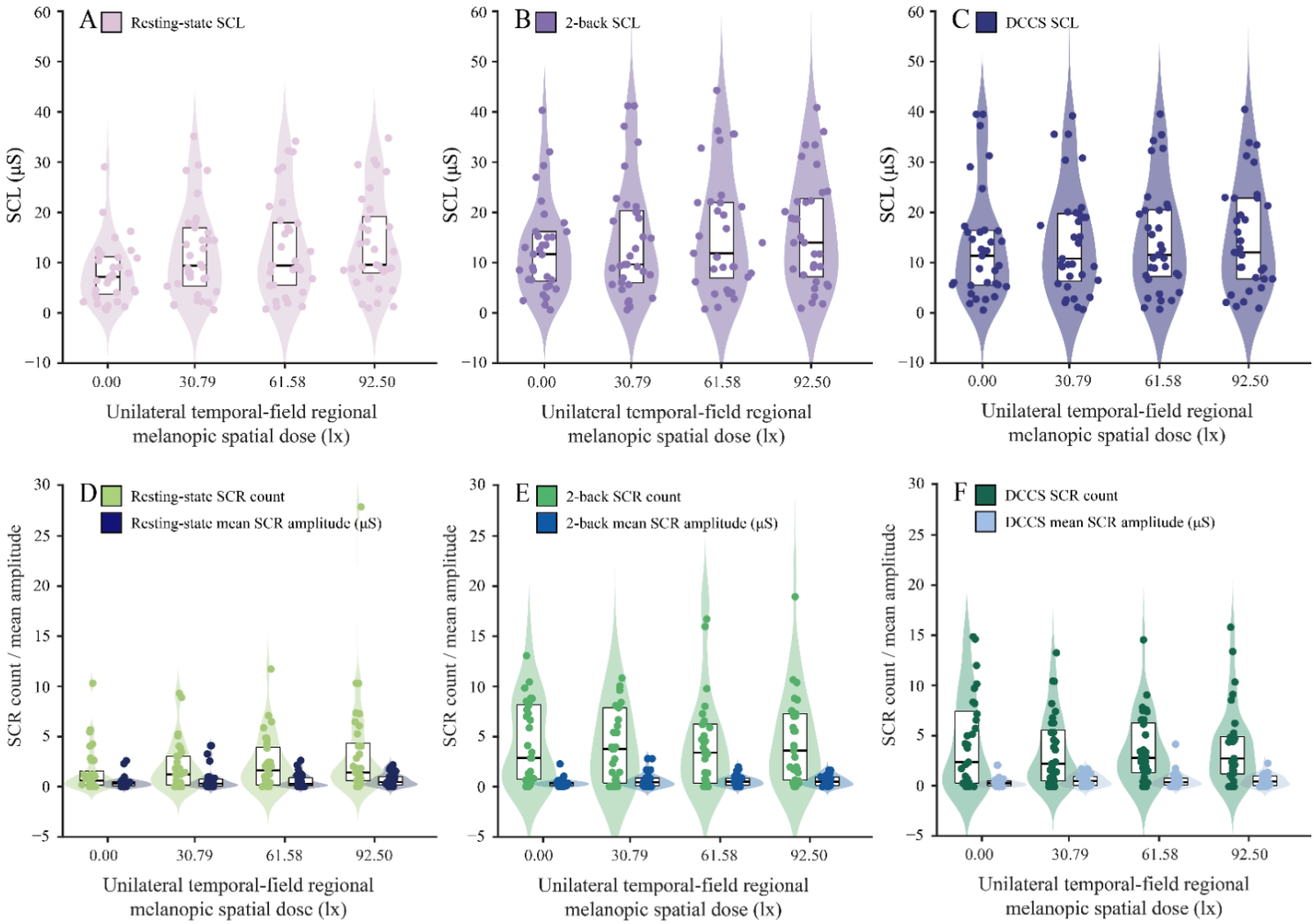


Figure 5

Electrodermal responses across the four regional melanopic spatial-dose conditions.Skin conductance level (SCL) distributions are shown during (A) resting-state, (B) 2-back, and (C) DCCS stages. Skin conductance response (SCR) count and mean SCR amplitude are shown during (D) resting-state, (E) 2-back, and (F) DCCS stages. Violin distributions, individual observations, and embedded box summaries illustrate between-condition variation at regional melanopic spatial doses of 0.00, 30.79, 61.58, and 92.50 lx.

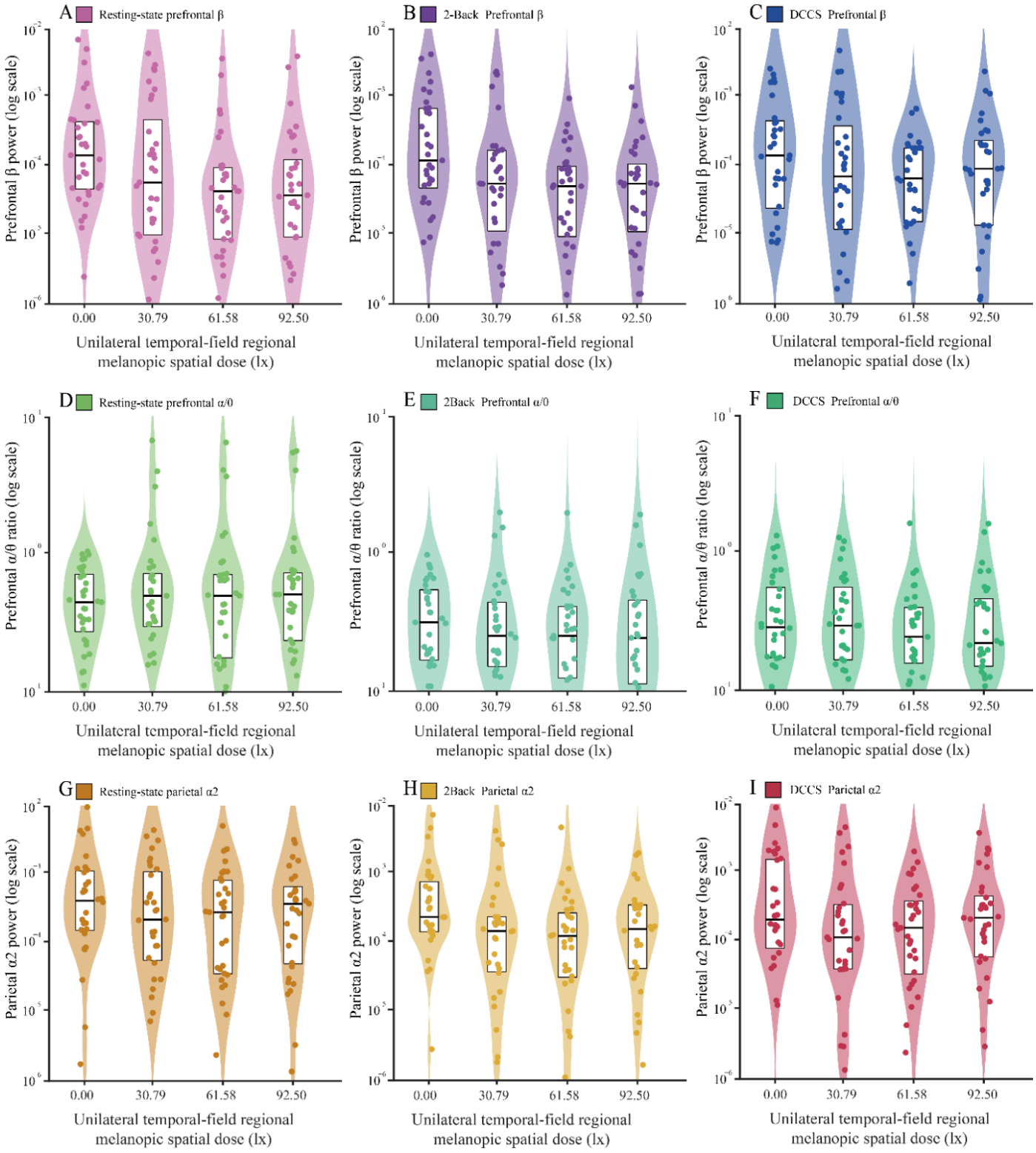


Figure 6

EEG responses across the four regional melanopic spatial-dose conditions Prefrontal β power is shown during (A) resting-state, (B) 2-back, and (C) DCCS stages; the prefrontal α/θ ratio during (D–F) the corresponding three stages; and parietal α2 power during (G–I) the corresponding three stages. Distributions are shown for regional melanopic spatial doses of 0.00, 30.79, 61.58, and 92.50 lx. Violin distributions, individual observations, and embedded box summaries illustrate the condition-level data. Prefrontal β power, the prefrontal α/θ ratio, and parietal α2 power are displayed on logarithmic scales as shown in the figure.

Supplementary Files

This is a list of supplementary files associated with this preprint. Click to download.

- SupplementaryTableS1S3.pdf